Am J Physiol Endocrinol Metab 287: E1008–E1018, 2004.
First published July 20, 2004; doi:10.1152/ajpendo.00008.2004.

Taurine increases glucose sensitivity of UCP2-overexpressing β-cells by ameliorating mitochondrial metabolism

Jin Han,[4]* Jae Hoon Bae,[1]* So-Yeon Kim,[1] Hyun-Young Lee,[1] Byeong-Churl Jang,[2] In-Kyu Lee,[2] Chi-Heum Cho,[2] Jeong-Geun Lim,[2] Seong-Il Suh,[2] Taeg-Kyu Kwon,[2] Jong-Wook Park,[2] Shin Young Ryu,[3] Won-Kyung Ho,[3] Yung-E Earm,[3] and Dae-Kyu Song[1,2]

[1]*Department of Physiology,* [2]*Chronic Disease Research Center, Keimyung University School of Medicine, Daegu 700-712;* [3]*Department of Physiology, College of Medicine, Seoul National University, Seoul 110-799; and* [4]*Department of Physiology and Biophysics, College of Medicine, Inje University, Busanjin-Gu, Busan 614-735, Korea*

Submitted 7 January 2004; accepted in final form 18 July 2004

Han, Jin, Jae Hoon Bae, So-Yeon Kim, Hyun-Young Lee, Byeong-Churl Jang, In-Kyu Lee, Chi-Heum Cho, Jeong-Geun Lim, Seong-Il Suh, Taeg-Kyu Kwon, Jong-Wook Park, Shin Young Ryu, Won-Kyung Ho, Yung-E Earm, and Dae-Kyu Song. Taurine increases glucose sensitivity of UCP2-overexpressing β-cells by ameliorating mitochondrial metabolism. *Am J Physiol Endocrinol Metab* 287: E1008–E1018, 2004. First published July 20, 2004; doi:10.1152/ajpendo.00008.2004.—A low-taurine diet during fetal or early postnatal life causes abnormal pancreatic β-cell development. Tissue and plasma taurine concentrations can also be low in diabetic patients. We examined the effect of taurine on impaired glucose responses in diabetic rat β-cells adenovirally overexpressing uncoupling protein (UCP)2, which is upregulated in obesity-related type 2 diabetes. We found that taurine pretreatment restored the ATP-to-ADP (ATP/ADP) ratio and glucose-stimulated insulin secretion in UCP2-infected islets. ATP-sensitive K^+ channel sensitivity to dihydroxyacetone, another insulin secretagogue, was similar in both UCP2-infected and control β-cells. In freshly isolated mitochondria from UCP2-overexpressing insulin-secreting (INS)-1 β-cells, methyl pyruvate-mediated mitochondrial Ca^{2+} increase was significantly ameliorated by taurine. A mitochondrial Ca^{2+} uniporter blocker, ruthenium red, inhibited the action of taurine. This study suggests that taurine enhances the glucose sensitivity of UCP2-overexpressing β-cells, probably by increasing mitochondrial Ca^{2+} influx through the Ca^{2+} uniporter, thereby enhancing mitochondrial metabolic function and increasing the ATP/ADP ratio.

insulin; ATP-sensitive K^+ channel; mitochondrial Ca^{2+}; ATP-to-ADP ratio; pancreatic islets; uncoupling protein 2

MITOCHONDRIAL OXIDATIVE METABOLISM plays a pivotal role in the generation of signals coupling glucose recognition to insulin secretion in pancreatic β-cells (29). The main physiological secretagogue, glucose, is metabolized in pancreatic β-cells, generating NADH (38) and $FADH_2$ (28). Electrons donated from NADH move down the electron transport chain, causing protons to be pumped out of the mitochondrial matrix by complexes I (NADH-ubiquinone oxidoreductase), III (ubiquinone-cytochrome-*c* oxidoreductase), and IV (cytochrome oxidase), creating a proton electrochemical gradient. $FADH_2$ donates electrons to complex II. The reentry of protons through ATP synthase generates ATP from ADP (40), thus increasing the ATP-to-ADP (ATP/ADP) ratio, resulting in the closure of ATP-sensitive K^+ (K_{ATP}) channels and plasma membrane depolarization. This leads to Ca^{2+} influx through voltage-gated Ca^{2+} channels and a rise in cytosolic Ca^{2+}, which is the main trigger for insulin secretion (2).

Prolonged exposure of β-cells to high glucose concentrations generates oxidative stress, resulting in β-cell dysfunction and ultimately cell death (47). Uncoupling protein (UCP)2 (8), a member of the mitochondrial inner membrane carrier family, catalyzes a proton leak, thereby hypopolarizing the mitochondrial membrane potential and reducing cellular ATP content (7). UCP2 expression in β-cells is increased by oxidative stress, suggesting that UCP2 uncoupling activity is physiologically important for β-cell defense against oxidants (25). However, glucose-stimulated insulin secretion (GSIS), critical for maintaining normal blood glucose levels, is suppressed when UCP2 is overexpressed in isolated islets (7) or when endogenous UCP2 is upregulated by long-term exposure (>48 h) of β-cells or insulin-secreting (INS)-1 β-cells to high glucose (36) or free fatty acids (5, 7, 14, 22, 49). In contrast, mice lacking UCP2 secrete more insulin and recover GSIS (48). Despite its important physiological role, UCP2 can also play a pathogenic role in the development of type 2 diabetes. Therefore, it would be useful to investigate mechanisms that ameliorate GSIS in a UCP2-overexpression model to develop new anti-diabetic therapies.

The β-amino acid taurine (2-aminoethanesulfonic acid) has many physiological functions in various cell types (20). An important function of taurine is to stimulate Ca^{2+} uptake, and this has been demonstrated in cardiac sarcolemma (42) and rat retina mitochondrial membrane preparations (26). Taurine is reported to potentiate Ca^{2+} sequestration via the Ca^{2+} uniporter embedded on the inner membrane in mitochondria isolated from rat liver (34) and neurons (21). Because intramitochondrial Ca^{2+} concentration ($[Ca^{2+}]_m$) has been observed to activate several dehydrogenases coupled to the Krebs or tricarboxylic acid cycle (30, 39), determinants of $[Ca^{2+}]_m$ may be critical for controlling β-cell metabolic rate. Blocking of $[Ca^{2+}]_m$ efflux in pancreatic β-cells with CGP-37157, a mitochondria-specific Na^+/Ca^{2+} exchanger antagonist, has been recently shown to increase GSIS (23). Despite the important role of taurine in $[Ca^{2+}]_m$, its influence has not been emphasized in the $[Ca^{2+}]_m$ dynamics in β-cells.

Previously, the effect of taurine on β-cells has been investigated mainly in vivo, because short-term taurine treatment in

* J. Han and J. H. Bae contributed equally to this study.

Address for reprint requests and other correspondence: D.-K. Song, Dept. of Physiology, Keimyung Univ. School of Medicine, 194, Dongsan-Dong, Jung-Gu, Daegu 700-712, Korea (E-mail: dksong@kmu.ac.kr).

The costs of publication of this article were defrayed in part by the payment of page charges. The article must therefore be hereby marked "*advertisement*" in accordance with 18 U.S.C. Section 1734 solely to indicate this fact.

normally functioning β-cells in vitro has produced controversial results (9, 10, 45). In the present study, we used UCP2-overexpressing β-cells (7, 8, 16) to investigate more clearly the effect of taurine in short-term primary cultures and to elucidate the relationship between taurine and UCP2-induced impaired glucose sensitivity. We demonstrate that taurine ameliorates the ATP/ADP ratio in β-cells with high UCP2 levels, thereby increasing GSIS, probably by improving $[Ca^{2+}]_m$ sequestration through the Ca^{2+} uniporter.

MATERIALS AND METHODS

Collection of pancreatic islets, single islet cells, and INS-1 β-cells. Islets of Langerhans were isolated from the pancreata of male Sprague-Dawley rats, each weighing 200–250 g, by a collagenase digestion technique as described previously (35). All procedures were approved by the Institutional Animal Care and Use Committee at the Dongsan Medical Institute for Life Sciences in Daegu, Korea. Prepared islets or single islet cells were incubated in RPMI-1640 media with 11.1 mM glucose in a humidified atmosphere of 5% CO_2 in air at 37°C. INS-1 β-cells were grown in monolayer cultures, as previously described (1), in RPMI medium containing 11.1 mM glucose supplemented with 10 mM HEPES, 2 mM glutamine, 1 mM sodium pyruvate, 50 μM β-mercaptoethanol, and the antibiotics in the same incubator as the β-cells. All studies were performed on INS-1 between passages 20 and 30 in appropriate test protocols. No FBS was applied during experimental cultures of INS-1 β-cells, pancreatic islets, and islet cells to avoid possible contamination of taurine. After adenovirus infection, these cells were cultured in RPMI medium containing 3 or 5 mM glucose as indicated in the text.

Overexpression of UCP2. A full-length human UCP2 (hUCP2/pBS) was subcloned into the *Hin*dIII/*Bam*HI site of the pAd-YC2 shuttle vector (11). UCP2/pAd-YC2 and rescue vector pJM17 (17) were cotransfected into human embryonic kidney (HEK)-293 cells with Tfx-20 (Promega, Madison, WI), according to the manufacturer's protocol. After 12 days, recombinants were identified using PCR. The recombinants were amplified in HEK-293 cells and purified in a cesium chloride density gradient. Control adenovirus, Ad-Null, was made and identified using the same method. INS-1 or islet cells were infected with Ad-Null [multiplicity of infection (MOI) = 100 or 500] or UCP2 adenoviruses (Ad-UCP2; MOI = 10, 100, or 500) (46). The adenovirus titer was 3.5×10^9 plaque-forming units (PFU), and one islet was assumed to have 10^3 β-cells (7). Virus-treated dishes were incubated for 2 h at 37°C and then washed with RPMI medium. INS-1 and islet cells were maintained for at least 48 h after infection, after which time experimental data were collected.

Subcellular fractionation. INS-1 β-cells were initially infected with 100 MOI of Ad-UCP2 or Ad-Null for 24 h and then treated with 3 or 15 mM glucose for an additional 48 h. Cells were then washed with PBS and lysed in *buffer A* [0.25 M sucrose, 30 mM Tris·HCl (pH 7.9), 1 mM EDTA, 0.5% Nonidet P-40, and protease inhibitor cocktails (×1)] along with short homogenization in a tissue grinder. Cells were then centrifuged at low speed for 5 min. The supernatant was further centrifuged at 14,000 *g* for 45 min. The pellet was washed with *buffer A* and lysed in *buffer B* (*buffer A* plus 3.6% Triton X-100) with sonication (35 strokes). The lysate was then centrifuged at 14,000 *g* for 15 min. The resultant supernatant was saved as Triton X-100-soluble fraction. The remaining pellet was washed with *buffer B* and lysed in *buffer C* (*buffer B* plus 1% SDS) with sonication (35 strokes). After centrifugation at 14,000 *g* for 15 min, the supernatant was saved as Triton X-100-insoluble fraction. The protein concentration of each fraction was determined.

Western blot analysis. INS-1 β-cells infected with Ad-UCP2 (10, 100, or 500 MOI) or Ad-Null (500 MOI only) for 48 h were washed and lysed in a buffer [50 mM Tris·HCl (pH 7.4), 150 mM NaCl, 1% Triton X-100, 1% SDS, 1% Nonidet P-40, 1 mM EDTA, 200 nM aprotinin, 20 μM leupeptin, 50 μM phenanthroline, and 280 μM benzamidine-HCl]. After centrifugation, the supernatant was collected, and the protein concentration was determined. Equal amounts of protein were resolved by 10% SDS-PAGE and transferred onto a nitrocellulose membrane (Millipore, Bedford, MA). The membrane was washed with Tris-buffered saline (TBS; 10 mM Tris, 150 mM NaCl) containing 0.05% Tween 20 (TBST) and blocked in TBST containing 5% nonfat dried milk. The membrane was incubated with antibodies of UCP2 (1:1,000; Alpha Diagnostic International, San Antonio, TX), prohibitin (1:1,000; NeoMarkers, Fremont, CA), or actin (1:10,000; Sigma, St. Louis, MO). After wash, the membrane was continuously incubated with appropriate secondary antibodies coupled to horseradish peroxidase and developed in enhanced chemiluminescence Western detection reagents.

Measurement of insulin secretion and insulin content in islets. Insulin secretion from islets was measured by RIA by use of the batch incubation method. The islets were preincubated for 1 h at 37°C in a modified Krebs-Ringer bicarbonate (KRB) buffer with 0.1% BSA and no glucose. Ten islets were then placed into each well of a 48-well plate containing glucose at the concentrations indicated. After incubation for 1 h at 37°C, an aliquot was taken from each well and centrifuged (700 *g*, 5 min), and the supernatant (200 μl) was carefully collected and stored (−20°C). To determine insulin content, the remaining islet pellet was washed in 400 μl of RPMI-1640 medium and lysed in 150 μl of ice-cold lysis buffer (50 mM HEPES, 0.1% Triton X-100, 1 μM phenylmethylsulfonyl fluoride, 10 μM E-64, 10 μM pepstatin A, 10 μM tosyl-L-lysine chloromethyl ketone, and 100 μM leupeptin; pH 8.0). After sonication and centrifugation (10,000 *g*, 2 min), the resultant supernatant was assayed for final insulin content (expressed as ng/ng DNA). Total islet insulin content was calculated by adding insulin secreted into the supernatant plus that remaining in the islet pellet. Percentage of islet insulin content secreted was calculated for each data point to eliminate variance caused by islet size and hence insulin content (7). Aliquots of the islet homogenates were also used for islet DNA quantification with DNeasy Tissue Kit (Qiagen, Valencia, CA). Rat insulin assay kits were purchased from Linco Research (St. Charles, MO). The mean from three consecutive batches with the same condition was taken as one data point. The number of data points (*n*) was obtained in at least three separate experiments.

Recording of single K_{ATP} channel activity. The cell-attached configuration of the conventional patch-clamp technique was used. Patch pipettes had a resistance of 3–5 MΩ. The single-channel currents were recorded using an Axopatch 200B patch-clamp amplifier (Axon Instruments, Forster, CA) and later analyzed with pClamp 8.2 software (Axon). Data were filtered at 1 kHz and sampled at 5 kHz. The channel activity was compared by use of the channel open probability (P_o) calculated from the following formula

$$P_o = \left(\sum_{j=1}^{N} t_j \cdot j \right) / (T_d \cdot N) \quad (1)$$

where t_j is the time spent at current levels corresponding to $j = 0, 1, 2, \ldots N$ channels in the open state; T_d is the duration of the recording; and N is the number of channels active in the patch. The number of channels in a patch was estimated by dividing the maximum current observed in the control solution by the mean unitary current amplitude. The relative channel activity in the presence of glucose was described as P_o/P_{oc}, where P_{oc} is the P_o recorded during the 30 s just before administration of glucose. During experiments, single islet cells on a cover glass (10 mm × 2 mm) were bathed in a solution composed of (in mM) 137 NaCl, 5.6 KCl, 1.2 $MgCl_2$, 2.6 $CaCl_2$, and 10 HEPES, adjusted to pH 7.4 with NaOH. The pipette solution contained (in mM) 140 KCl, 1.2 $MgCl_2$, 2.6 $CaCl_2$, and 10 HEPES, adjusted to pH 7.4 with KOH. The experiments were done at room temperature (20–22°C).

ATP and ADP measurements. ATP and ADP were assayed by luciferase measurement (Sigma) according to the manufacturer's protocol. ATP was assayed directly. For ADP measurements, ATP was first hydrolyzed to AMP with the use of ATP-sulfurylase. After inactivation of the sulfurylase, ADP was converted to ATP with pyruvate kinase and phosphoenolpyruvate and was quantified by luciferase measurement (41). Islets were starved for 2 h in glucose-free KRB buffer before 15-min exposure at 37°C to indicated concentrations of glucose.

Measurement of cytosolic Ca^{2+} concentration. Microfluorescent imaging of cytosolic Ca^{2+} concentration ($[Ca^{2+}]_c$) was performed on single islet cells loaded with the Ca^{2+} indicator dye fura-2 AM. Some of the procedures used in Ca^{2+} imaging in this experiment have been previously described (3). Fura-2 AM (3 μM) was added to islet cells, which were cultured on a coverslip (25 mm in diameter) and bathed in PBS at room temperature for 30 min followed by a 30-min wash in dye-free PBS to allow esterase conversion to free fura-2. A coverslip was placed on the stage of an inverted microscope, and imaging was performed with an InCa dual-wavelength system (Intracellular Imaging, Cincinnati, OH). Each experimental data point represents the mean $[Ca^{2+}]_c$ calculated from at least 20–30 individually measured cells from three separate cultures. All imaging experiments were done at room temperature.

Immunofluorescence and confocal laser scanning microscopy imaging. Indirect immunofluorescence was carried out to determine colocalization of UCP2 and cytochrome-*c* oxidase (COX) in INS-1 β-cells. Cells were fixed in 4% formaldehyde in PBS, permeabilized in 0.075% Triton X-100, and blocked in 2 mg/ml BSA and 0.1% Tween-20 for 1 h at room temperature. Primary antibody incubations were performed for 1 h at room temperature in 2 mg/ml of BSA and 0.1% Tween-20 plus antibodies at the following dilutions. Rabbit antibody against UCP2 (Alpha Diagnostic) was used at a dilution of 1:1,000, and mouse antibody against COX (Molecular Probes, Eugene, OR) was used at a dilution of 1:200. Antigen-antibody complexes were visualized with Alexa Fluor 488-conjugated Zenon rabbit IgG labeling kit (Molecular Probes) and Alexa Fluor 568-conjugated Zenon mouse IgG labeling kit (Molecular Probes). Cells were mounted on slides in ProLong Antifade (Molecular Probes). Confocal images were collected with the use of an LSM-510 META confocal microscope system (Carl Zeiss, Jena, Germany) equipped with a krypton-argon Omnichrome laser, with excitation wavelengths of 488 nm for the detection of Alexa Fluor 488 and 578 nm for Alexa Fluor 568. They were visualized under an inverted microscope (Axiovert 200 M BP, Carl Zeiss) at ×200, ×400, and ×630 with the appropriate laser lines and filter sets. Images were analyzed using LSM-510 META software (release 3.2; Carl Zeiss).

Preparation of mitochondria and $[Ca^{2+}]_m$ measurement. Mitochondria were collected and purified from individual INS-1 β-cells by discontinuous Percoll gradient purification. Individual INS-1 β-cells were homogenized in homogenization buffer with the use of a Dounce homogenizer before being centrifuged (3 min, 1,300 *g*, 4°C) in a swing-out rotor. The supernatant was then centrifuged (10 min, 21,000 *g*, 4°C) in an angle rotor. The pelleted cells were resuspended in 15% Percoll solution, layered in a tube that contained 23 and 40% Percoll solution in the same homogenization buffer, and centrifuged (5 min, 31,000 *g*, 4°C). Mitochondria were collected (at the lowest interface band), washed, and diluted in hypertonic solution. All procedures were carried out on ice, and all implements were cooled in a refrigerator before use. To assess the purity of the mitochondrial preparation, samples were stained with the mitochondria-specific red fluorescent probe MitoTracker Red CMXRos. As a negative control, samples were stained with the endoplasmic reticulum marker ER-Tracker Blue-White DPX.

$[Ca^{2+}]_m$ was determined by use of the fluorescent Ca^{2+} indicator fura-2. Freshly isolated mitochondria were dispersed in a cytosol-like solution and energized by the addition of 5 mM malate and 5 mM glutamate. Mitochondria were loaded with fura-2 AM (3 μM) for 60 min on ice under continuous stirring. The loaded mitochondria were then washed twice with fresh solution, diluted 1:10, placed in ultraviolet-grade fluorometric cuvettes (Spectrocel), and continuously stirred at room temperature. Sulfinpyrazone (250 μM) was added to all solutions to prevent dye leakage. For the fluorometric measurement of $[Ca^{2+}]_m$, we used a delta-SCAN Photon Technology International Spectrofluorometer System (PTI, South Brunswick, NJ). Fluorescence ratios were monitored with dual excitation at 340 and 380 nm (F_{340}/F_{380}) and emission at 510 nm.

In mitochondrial preparation, the homogenization buffer contained 320 mM sucrose, 1 mM K-EDTA, 0.1% BSA, and 10 mM Tris·HCl, titrated to pH 7.2 with KOH. The wash solution contained 150 mM KCl, 1 mM K-EGTA, 0.1% BSA, and 20 mM K-HEPES, titrated to pH 7.2 with KOH. The hypertonic solution contained 750 mM KCl, 1 mM K-EGTA, and 100 mM K-HEPES, titrated to pH 7.2 with KOH. As a measurement of $[Ca^{2+}]_m$, a cytosol-like solution contained 150 mM KCl, 2 mM KH_2PO_4, 5 mM $MgCl_2$, 10 mM HEPES, 0.5 mM EGTA, and 500 nM $CaCl_2$, titrated to pH 7.2 with KOH. Fluorescent probes were purchased from Molecular Probes. All other reagents were obtained from Sigma.

Statistical analysis. Data are expressed as means ± SE. Statistical significance was evaluated by unpaired Student's *t*-test when only two groups were involved. Multiple comparisons were made by ANOVA. $P < 0.05$ was considered significantly different.

RESULTS

Adenoviral vector-mediated overexpression of UCP2 in INS-1 β-cells. To endogenously overexpress UCP2, INS-1 β-cells were infected with Ad-UCP2 (10, 100, or 500 MOI) or Ad-Null (500 MOI only) in the presence of low glucose (3 mM) for 48 h. As shown in Fig. 1*A*, there was little expression of UCP2 in Ad-Null-infected INS-1 cells (*lane 1*), whereas there was a concentration-dependent increase of UCP2 expression in INS-1 β-cells when the concentrations of Ad-UCP2 were increased (*lanes 2–4*). For example, ~30-fold induction of UCP2 protein was seen in INS-1 β-cells that were infected with 100 MOI of Ad-UCP2 compared with endogenous UCP2 protein level in Ad-Null-infected cells, as measured by densitometer (data not shown).

It has been previously reported that, when UCP3 protein, another member of the UCPs, is adenovirally overexpressed in muscle-derived L6 cells, this protein mainly localizes to the mitochondria, and UCP3 protein localized to the mitochondria is insoluble by 3.6% Triton X-100, a strong nonionic detergent (18). To examine whether UCP2, when adenovirally overexpressed in INS-1 β-cells, also localizes to the mitochondria and whether UCP2 localized into the mitochondria is elutable by Triton X-100, biochemical subcellular fractionation and subsequent UCP2 Western analysis were carried out in INS-1 β-cells infected with 100 MOI of Ad-Null or Ad-UCP2 and then further grown in the presence of 15 mM high glucose for 48 h. The data of UCP2 Western analysis showed that, when induced by high glucose in Ad-Null INS-1 β-cells or by Ad-UCP2 infection in INS-1 β-cells, UCP2 localized to the mitochondria (data not shown). However, unlike UCP3, a majority of mitochondrial UCP2 protein was readily elutable by 3.6% Triton X-100 (Fig. 1*B*).

Expression of UCP2 protein in INS-1 β-cells and mitochondria. To confirm that the transfection of UCP2 using adenovirus had succeeded in the mitochondria, we performed dual-immunofluorescent labeling studies to detect colocalization within fixed Ad-UCP2-infected INS-1 β-cells. We used a

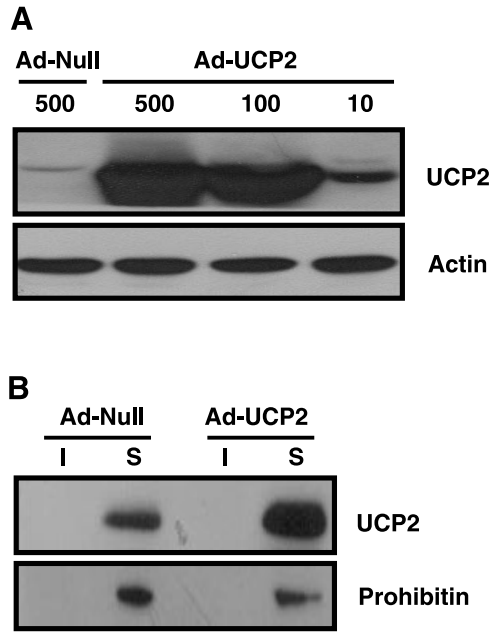

Fig. 1. Overexpression and cellular localization of uncoupling protein (UCP)2 in insulin-secreting (INS)-1 β-cells after high glucose administration or human UCP2 gene-delivering adenovirus infection. *A*: INS-1 β-cells were infected with Ad-UCP2 [multiplicity of infection (MOI) = 10, 100, or 500] or Ad-Null (500 MOI only) in the presence of 3 mM glucose for 48 h. Total cell lysates were prepared and analyzed for UCP2 or actin Western blot. *B*: INS-1 β-cells were infected with either 100 MOI Ad-UCP2 or Ad-Null for 24 h in the presence of 3 mM glucose. At 24 h postinfection, cells were further exposed to 15 mM glucose for an additional 48 h, after which a mitochondrial fraction was isolated. To assess the solubility of mitochondrial UCP2 protein by Triton X-100, the isolated mitochondrial fraction was further extracted with a high concentration of Triton X-100 (3.6%). Triton X-100 (3.6%)-insoluble (I) and -soluble (S) mitochondrial protein extracts were analyzed for Western blot for UCP2 or prohibitin, a Triton X-100-soluble mitochondrial protein.

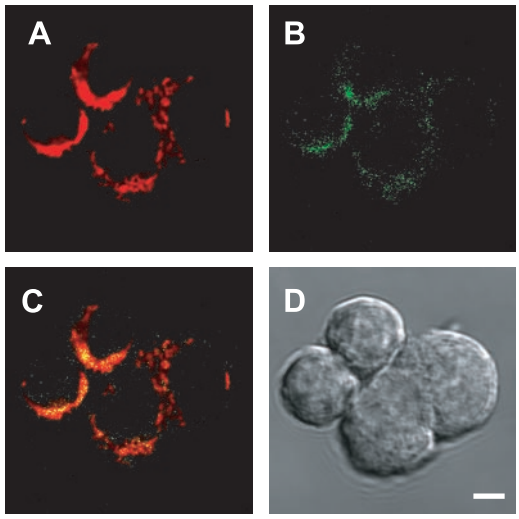

Fig. 2. Expression of UCP2 protein in adenoviral-infected INS-1 β-cells and mitochondria. For immunofluorescence analysis of UCP2 protein in Ad-UCP2-infected INS-1 β-cells, the cells were fixed, permeabilized, and stained for cytochrome-*c* oxidase (COX; *A*) and UCP2 (*B*) using mouse anti-COX and rabbit anti-UCP2 antibody. Confocal images were collected with identical iris settings. Overlay of red and green channels (*C*) was created to examine the degree of colocalization. Yellow or orange areas represent regions of colocalization. *D*: transmitted light with differential interference contrast optics. All images were captured at ×630 magnification. Scale bar = 5 μm.

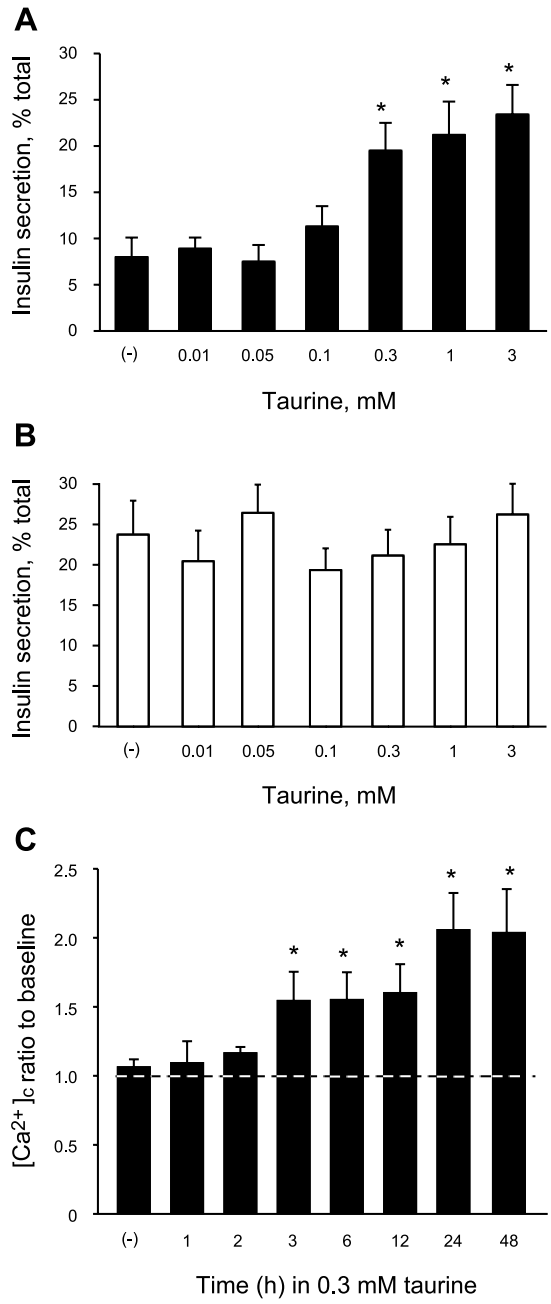

Fig. 3. Determination of the optimal concentration and duration for taurine pretreatment. *A*: changes in glucose-stimulated insulin secretion (GSIS) in Ad-UCP2-infected islets after 24-h pretreatment with various concentrations of taurine. Percentages of total insulin content secreted for each group during 1-h incubation in 15 mM glucose are shown. Symbols represent means ± SE; n = 3–6 for each mean. *$P < 0.05$ compared with taurine-free control. *B*: changes in GSIS in Ad-Null-infected islets after 24-h pretreatment with various concentrations of taurine. Symbols represent means ± SE; n = 3–6 for each mean. *C*: relative changes in glucose-stimulated cytosolic Ca^{2+} concentration ($[Ca^{2+}]_c$) increase in Ad-UCP2-infected islets after pretreatment for various times with 0.3 mM taurine. Symbols represent means ± SE obtained from normalization using the average $[Ca^{2+}]_c$ during the 5-min exposure to glucose and the average $[Ca^{2+}]_c$ during the 1 min before glucose application, with the dashed line indicating the level of $[Ca^{2+}]_c$ before glucose application in each group; n = 18–23 for each mean. *$P < 0.05$ compared with taurine-free control.

mouse antibody directed against COX (Fig. 2*A*), which has been described to be mitochondria located, in conjunction with a rabbit antibody directed against UCP2 (Fig. 2*B*). As shown in Fig. 2*C*, there was a colocalization between COX and UCP2, indicating that UCP2 localizes specifically to mitochondria.

Determination of the optimal concentration and duration for taurine pretreatment. We measured whether GSIS could be changed in Ad-Null- or Ad-UCP2-infected islets by pretreatment with taurine for 24 h. It has been previously shown that the infection of islets with adenovirus does not significantly affect insulin secretory capacity (50). GSIS induced by 15 mM glucose, expressed as a percentage of total islet insulin content released, was significantly increased by pretreatment with 0.3 mM taurine (Fig. 3*A*). We therefore used 0.3 mM taurine for the subsequent experiments. However, taurine pretreatment in the range of concentrations tested had no effect on GSIS in Ad-Null-infected islets (Fig. 3*B*). Second, we measured $[Ca^{2+}]_c$ in response to 10 mM glucose in Ad-UCP2-infected islet cells without or with 0.3 mM taurine pretreatment for various times (Fig. 3*C*). Taurine caused a significant glucose-stimulated $[Ca^{2+}]_c$ increase after 3 h of pretreatment. The increase reached a maximum at 24 h, which was used as the duration of pretreatment in the following experiments. During experiments, except for $[Ca^{2+}]_m$ measurements, 0.3 mM taurine was present in all solutions for the taurine group.

Effect of 0.3 mM taurine pretreatment for 24 h on GSIS and islet insulin content. As shown in Fig. 4*A*, there was no significant difference in islet insulin content when measured after 48-h incubation with 5 mM glucose in Ad-Null- or Ad-UCP2-infected islets in the absence or presence of 0.3 mM taurine. Exposing the islets to 15 mM glucose for 1 h showed a decrease of insulin secretory response in Ad-UCP2-infected islets (Fig. 4*B*; 31.7 ± 5.9 pg/ng DNA, $n = 6$, vs. 75.5 ± 6.2 in Ad-Null, $n = 6$, $P < 0.05$). Ad-UCP2-infected islets with taurine pretreatment (+T) exhibited remarkably ameliorated GSIS (60 ± 4.7 pg/ng DNA vs. Ad-UCP2 group, $n = 6$, $P < 0.05$). As expected, final insulin content after high glucose stimulation for 1 h was greater in taurine-free Ad-UCP2-infected islets (0.36 ± 0.04 ng/ng DNA, $n = 6$) than in the other three groups (Fig. 4*C*; 0.25 ± 0.03 ng/ng DNA in Ad-Null, 0.26 ± 0.03 in Ad-Null + T, $n = 6$, and 0.25 ± 0.02 in Ad-UCP2 + T groups). Fractional insulin secretion by high glucose was also significantly impaired in Ad-UCP2-infected islets (Fig. 4*D*; 8 ± 2.1% vs. 23.8 ± 4.2%, $P < 0.05$, in Ad-Null), but it was recovered in Ad-UCP2 + T islets (19.5 ± 3% vs. Ad-UCP2 group, $P < 0.05$). Basal insulin secretory capacity at 5 mM glucose did not significantly differ among the groups ($P > 0.05$). Simultaneous pretreatment with taurine and guanidinoethane sulfonate, a Na^+-dependent taurine transporter inhibitor, totally blocked the taurine action, implying that taurine has its effect within the cell, not on the external cell surface (data not shown).

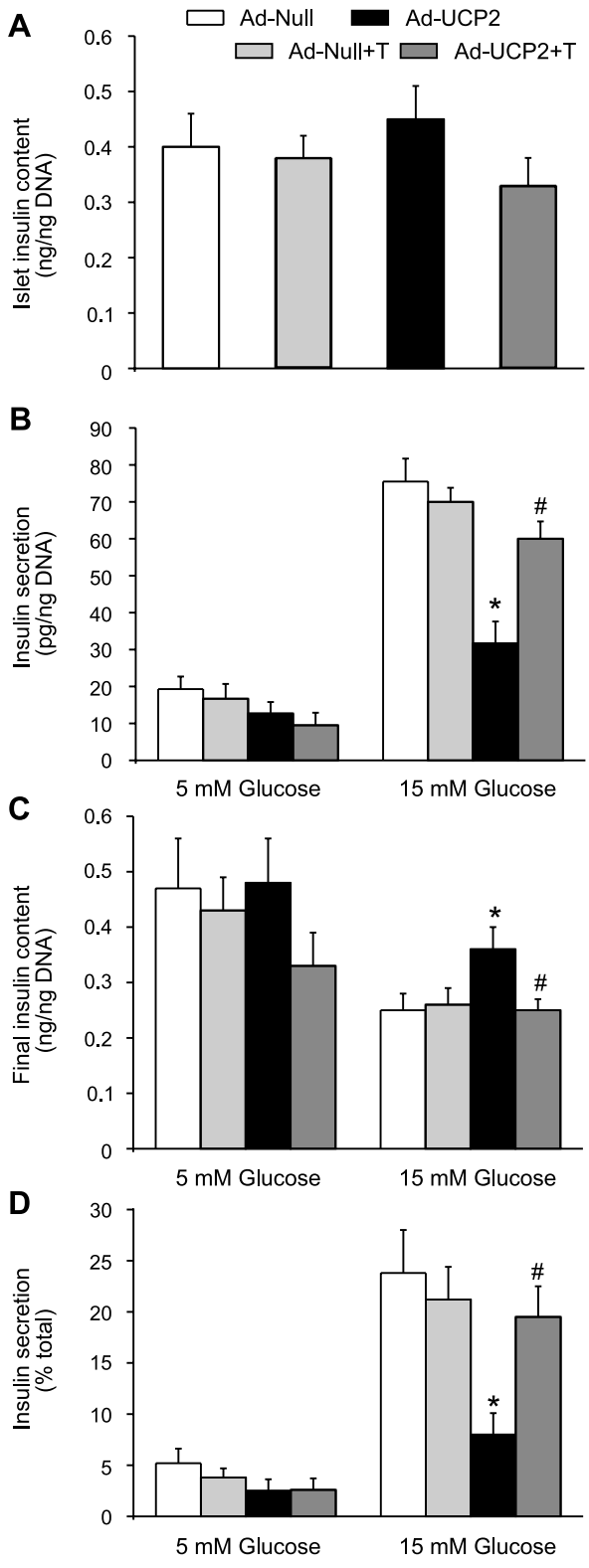

Fig. 4. Effect of taurine on insulin secretion and insulin content in adenovirus-infected islets. *A*: islet insulin contents obtained from Ad-Null- or Ad-UCP2-infected islets after 48-h incubation in 5 mM glucose in the absence or presence (+T) of taurine pretreatment. *B*: static insulin secretion from Ad-Null- or Ad-UCP2-infected islets in the absence or presence of taurine pretreatment. Islets of each group were incubated in 5 or 15 mM glucose for 1 h. *C*: final insulin contents obtained from corresponding islets in *B*. *D*: fractional insulin secretion expressed as a percentage of total insulin content secreted. Total insulin content is the sum of final insulin content and corresponding secreted insulin. Symbols represent means ± SE. Insulin content and insulin secretion were corrected using the islet DNA content. Islets taken after 1-h incubation for insulin secretion were retrieved and extracted for insulin content measurement. The same islet homogenates were used to measure islet DNA content. *$P < 0.05$ compared with Ad-Null-infected group; #$P < 0.05$ compared with Ad-UCP2-infected group.

Effect of taurine on the $[Ca^{2+}]_c$ response to high glucose stimulation. Resting $[Ca^{2+}]_c$ in the three groups (Ad-Null, Ad-UCP2, and Ad-UCP2 + T) at 3 mM glucose ranged from 50 to 100 nM. Application of high glucose (10 mM) through the bath solution elicited a gradual increase in $[Ca^{2+}]_c$ in Ad-Null-infected islet cells, with a time lag of ~10 s (Fig. 5*A*). The Ad-UCP2-infected islet cells showed almost no glucose-stimulated $[Ca^{2+}]_c$ elevation during the periods of the experiments, but, in taurine-pretreated UCP2-infected cells, the high glucose could elicit the increase in $[Ca^{2+}]_c$ (Fig. 5*B*). The $[Ca^{2+}]_c$ in the Ad-UCP2 group could be increased by the application of glibenclamide, a well-known blocker of the K_{ATP} channel, comparable with the response of the Ad-Null group (Fig. 5, *C* and *D*, respectively).

Effect of taurine on the glucose sensitivity of K_{ATP} channels. If pretreatment with taurine substantially makes it possible to induce a glucose-stimulated $[Ca^{2+}]_c$ increase in UCP2-overexpressing islet cells, the K_{ATP} channel sensitivity to glucose should also be increased to trigger membrane depolarization. In the cell-attached patch clamp mode, 10 mM glucose was added to the bath solution. The glucose sensitivity of K_{ATP} channels in Ad-UCP2-infected β-cells was considerably lower than that of Ad-Null-infected β-cells (Fig. 6). This reduced sensitivity to glucose significantly recovered with taurine pretreatment. Substitution of methylpyruvate for glucose, bypassing glycolysis, showed the same electrophysiological results as glucose (data not shown), suggesting that taurine exerts its effect downstream of glycolysis. The K_{ATP} channel sensitivity to glibenclamide in Ad-UCP2-infected β-cells remained normal (Fig. 6*B, trace 3*).

Effect of taurine on adenine nucleotide levels and the ATP/ADP ratio. ATP and ADP levels and the ATP/ADP ratio between Ad-Null and Ad-Null + T islets were not different either in basal glucose or in high glucose stimulation (Table 1). However, Ad-UCP2-infected islets exhibited remarkably lower ATP levels and ATP/ADP ratios and higher ADP levels compared with Ad-Null-infected control in both cases. These impaired parameters were significantly improved by the taurine pretreatment, showing more ATP and less ADP (thus higher ATP/ADP ratios), suggesting that a substantial amelioration of the ATP/ADP ratio occurred in Ad-UCP2 + T islets.

Dihydroxyacetone-induced K_{ATP} channel inhibition. Dihydroxyacetone (DHA) renders $FADH_2$ to complex II of the mitochondrial electron transport system directly through the glycerophosphate shuttle, bypassing the TCA cycle (43). To investigate the cause of reduced GSIS in UCP2-overexpressing islets, we examined the DHA-induced K_{ATP} channel inhibition in Ad-UCP2- and Ad-Null-infected β-cells. Our assumption

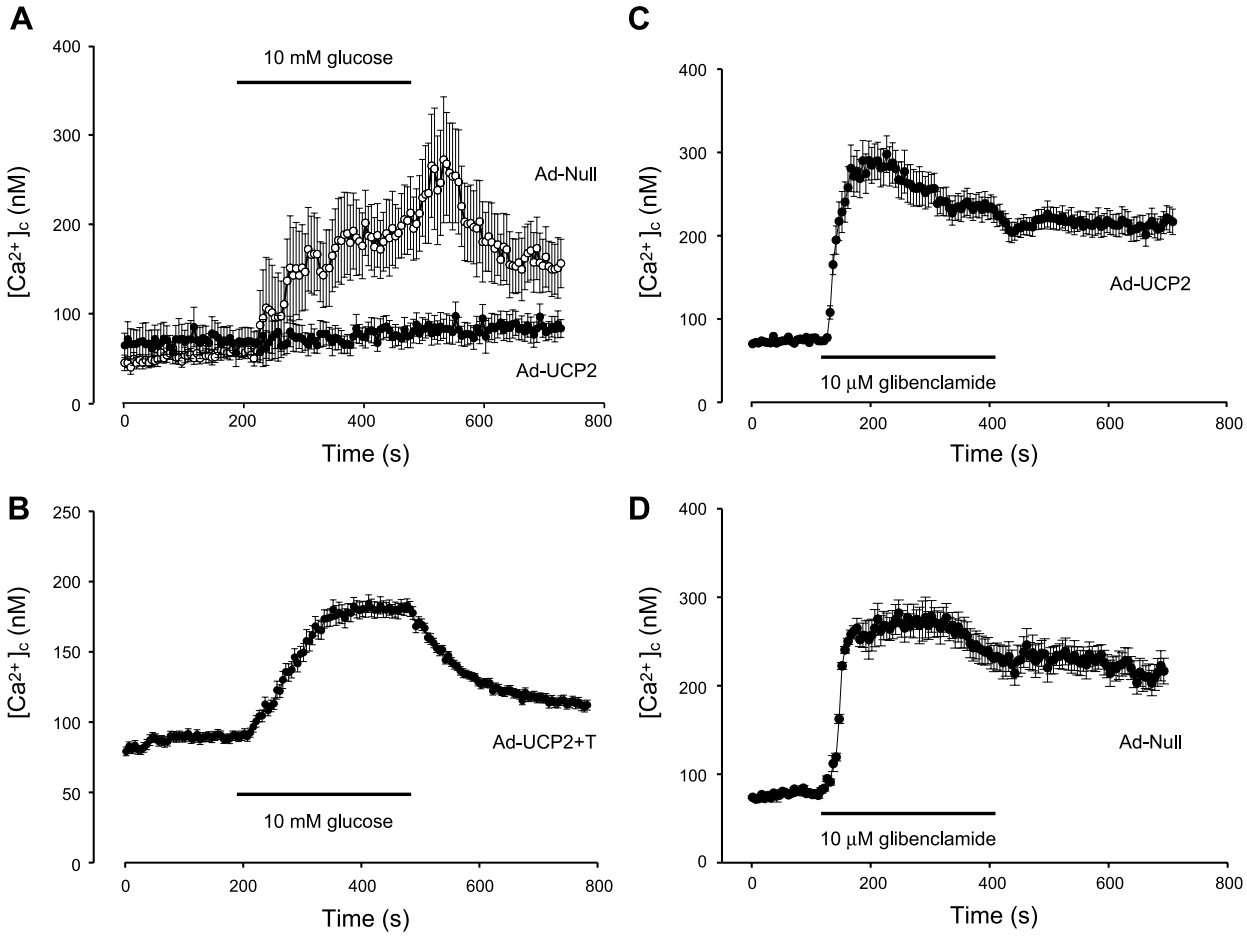

Fig. 5. Effect of taurine on $[Ca^{2+}]_c$ response to high glucose. *A*: glucose-stimulated $[Ca^{2+}]_c$ in Ad-Null- (n = 22) and Ad-UCP2-infected (n = 20) islet cells without taurine pretreatment. *B*: glucose-stimulated $[Ca^{2+}]_c$ in Ad-UCP2-infected islet cells with 0.3 mM taurine pretreatment for 24 h (n = 20). Glibenclamide-stimulated $[Ca^{2+}]_c$ in Ad-UCP2- (*C*; n = 23) and Ad-Null-infected (*D*; n = 17) islet cells without taurine pretreatment. Symbols represent means ± SE.

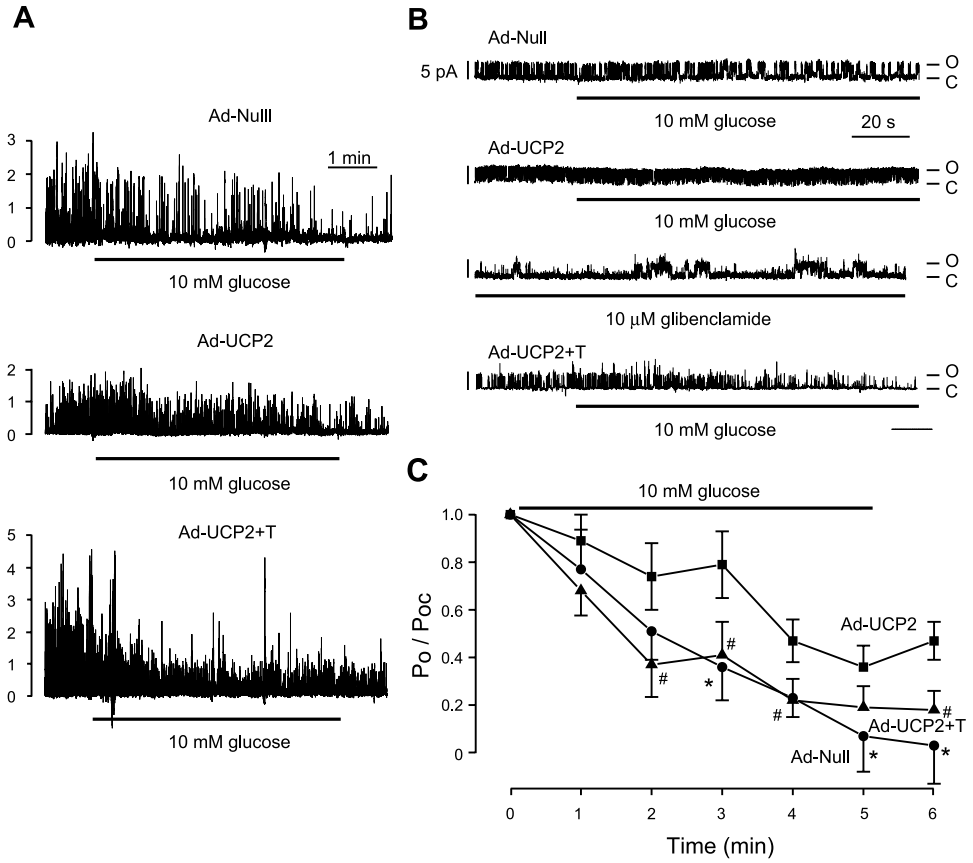

Fig. 6. Effect of taurine on glucose-stimulated ATP-sensitive K^+ (K_{ATP}) channel inhibition. *A*: effect of 10 mM glucose on K_{ATP} channel activity in Ad-Null, Ad-UCP2, and Ad-UCP2 + T β-cells. Cell-attached mode at a holding potential of 0 mV. *Vertical* scales indicate the no. of channels. *B*: representative traces in a larger time scale showing the effect of glucose on K_{ATP} channel activity in Ad-Null, Ad-UCP2, and Ad-UCP2 + T β-cells. Glibenclamide at 10 μM easily blocked the channels of the glucose-insensitive Ad-UCP2-infected β-cell. O, open state; C, closed state. *C*: time course of K_{ATP} channel inhibition by glucose in Ad-Null ($n = 5$), Ad-UCP2 ($n = 5$), and Ad-UCP2 + T ($n = 5$). Open probability (P_o) measured in the presence of 10 mM glucose was normalized relative to P_o measured immediately before exposure to glucose (P_{oc}). Symbols represent means ± SE. T, pretreatment with 0.3 mM taurine for 24 h. *$P < 0.05$ and #$P < 0.05$ compared with Ad-UCP2.

was that if K_{ATP} channel inhibition was normal in Ad-UCP2-infected β-cells, the sites responsible for the impairment of high glucose sensitivity, i.e., those responsible for reduced ATP production by Ad-UCP2 infection, could be within the TCA cycle upstream of the electron transport system. In fact, externally applied DHA in the cell-attached mode inhibited K_{ATP} channel activity in Ad-UCP2-infected β-cells to the same extent as in Ad-Null-infected controls (Fig. 7). The above finding revealed that the defect of GSIS in UCP2-overexpressing β-cells may be due to more than UCP2-mediated proton leak in response to incoming reducing equivalents; rather, it may be due to reduced metabolism of glucose metabolites in the TCA cycle secondary to UCP2 overexpression.

Table 1. *Effect of taurine on ATP levels and the ATP/ADP ratios in islets*

	Null	Null + T	UCP2	UCP2 + T
Glucose (3 mM)				
ATP, pM/islet	3.2±0.4	3.1±0.3	2.1±0.3*	2.5±0.3
ADP, pM/islet	4.3±0.6	3.7±0.4	5.0±0.4	3.8±0.5†
ATP/ADP ratio	0.7±0.2	0.8±0.2	0.4±0.1*	0.7±0.2†
Glucose (15 mM)				
ATP, pM/islet	4.8±0.5	4.7±0.4	2.4±0.3*	3.8±0.5†
ADP, pM/islet	3.0±0.6	2.8±0.4	4.8±0.5*	2.7±0.5†
ATP/ADP ratio	1.6±0.6	1.7±0.4	0.5±0.1*	1.4±0.6†

Values are means ±SE of 3 separate experiments. T, pretreatment with 0.3 mM taurine for 24 h; UCP, uncoupling protein; ATP/ADP ratio, ratio of ATP to ADP. *$P < 0.05$ compared with Null control; †$P < 0.05$ compared with UCP2.

Effect of taurine on methyl pyruvate-induced increases in $[Ca^{2+}]_m$. We hypothesized that taurine might increase $[Ca^{2+}]_m$ reduced by UCP2 overexpression, thereby potentiating mitochondrial glucose metabolism and leading to more glucose-

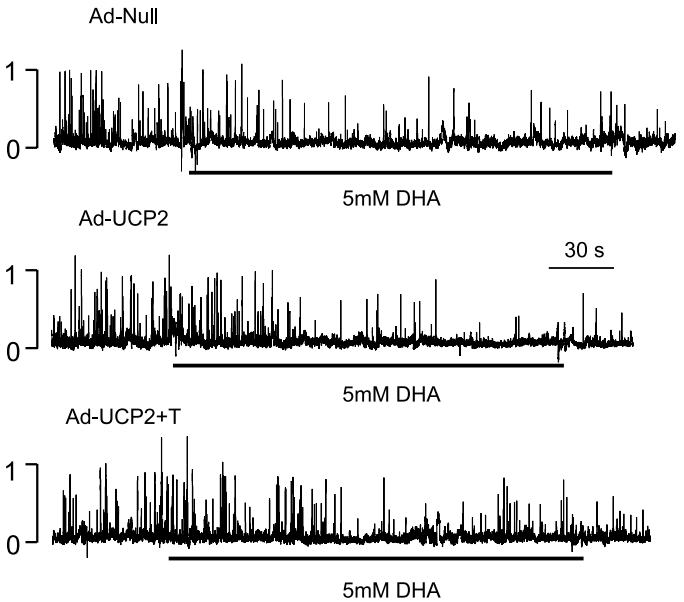

Fig. 7. Dihydroxyacetone (DHA)-stimulated K_{ATP} channel inhibition in Ad-Null control, Ad-UCP2, and Ad-UCP2 + T β-cells. Cell-attached mode at a membrane potential of 0 mV. DHA (5 mM) was applied to the bath solution where indicated. *Vertical* scales indicate the no. of channels. T, pretreatment with 0.3 mM taurine for 24 h.

stimulated ATP production and a higher ATP/ADP ratio in Ad-UCP2-infected β-cells. The effect of the tricarboxylic acid cyclic intermediate pyruvate, whose membrane permeability is increased by the ester binding of a methyl group, was tested in the fura-2-loaded mitochondria. This substrate has been shown to be a powerful stimulator of insulin secretion (24). Fluorescence ratio ($F_{340/380}$) of the mitochondria was measured from the mitochondrial suspensions and was regarded as a variable representing $[Ca^{2+}]_m$. The mean $F_{340/380}$ in the control condition was 1.1 ± 0.3 ($n = 15$). A concentration of 20 mM methyl pyruvate induced a rise in $[Ca^{2+}]_m$ (Fig. 8*A*). In addition, the increase in $[Ca^{2+}]_m$ induced by 20 mM methyl pyruvate was reversed by addition of 3 mM sodium azide, an inhibitor of the mitochondrial oxidative phosphorylation, indicating that the effect of methyl pyruvate on $[Ca^{2+}]_m$ was due to stimulation of the mitochondrial ATP production. We next compared the $[Ca^{2+}]_m$ levels in response to 20 mM methyl pyruvate in Ad-UCP2-infected mitochondria in the presence or absence of taurine. The peak $[Ca^{2+}]_m$ levels measured during exposure to methyl pyruvate were significantly lower in the Ad-UCP2 group ($P < 0.05$, Fig. 8*B*) than in the Ad-Null group (Fig. 8*A*). The methyl pyruvate-induced increase in $[Ca^{2+}]_m$ was significantly improved in the Ad-UCP2 + T group ($P < 0.05$, Fig. 8*C*). However, pretreatment with ruthenium red (10 μM), the mitochondrial Ca^{2+} uniporter blocker, totally blocked the methyl pyruvate-induced increase in $[Ca^{2+}]_m$ (Fig. 8*D*). The percent increases in $[Ca^{2+}]_m$ are 110 ± 20, 40 ± 10, and 85 ± 15% of baseline (before treatment of methyl pyruvate) in Ad-Null ($n = 7$), Ad-UCP2 ($n = 6$), and Ad-UCP2 + T ($n = 6$) groups, respectively (Fig. 8*E*).

Effects of the modulators for $[Ca^{2+}]_m$ influx or efflux mechanism on the enhanced GSIS by taurine. We tested modulators that affect pathways for the movement of Ca^{2+} in and out of the mitochondria to find out the mechanism critical for the taurine-mediated, glucose-stimulated $[Ca^{2+}]_m$ increase (19). The mitochondrial uptake of Ca^{2+} is mainly mediated by the Ca^{2+} uniporter, whereas Ca^{2+} efflux is controlled by both Na^+/Ca^{2+} and Ca^{2+}/H^+ antiporters in addition to the mitochondrial permeation transition pore (PTP). First, islets were pretreated with 10 μM cyclosporine A (CysA), a potent PTP blocker, for 1 h before high glucose stimulation (Fig. 9). The restoring action of taurine on insulin secretion in Ad-UCP2-infected islets was not abolished even in the presence of CysA (14 ± 2.4% total insulin content secreted vs. 7.6 ± 1.5% in Ad-UCP2 group, $P < 0.05$, $n = 6$). It was consistent with a report that CysA failed to block the enhancing effect of taurine on Ca^{2+} sequestration into rat liver mitochondria (34). Pretreatment with CGP-37157 (10 μM), a Na^+/Ca^{2+} exchanger antagonist (23), also did not modify the stimulatory action of taurine on GSIS (38 ± 5.1% vs. 21.6 ± 3.7% in Ad-UCP2 group, $P < 0.05$, $n = 6$). Finally, we introduced ruthenium red (10 μM) (3), the mitochondrial Ca^{2+} uniporter blocker, and found that it negatively regulated GSIS in Ad-Null-, Ad-Null + T-, and Ad-UCP2-infected islets. In Ad-UCP2-infected islets with taurine pretreatment, the effect of taurine on GSIS totally disappeared in the presence of ruthenium red (2.5 ± 0.6% vs. 2.9 ± 0.5% in Ad-UCP2-infected islets, $P > 0.05$, $n = 6$). Pretreatment of Ad-Null-infected islets with taurine had no significant effect on the insulin response of islets to the three different agents.

DISCUSSION

Type 2 diabetes can be aggravated by environmental factors such as low physical activity or hypercaloric glucose- or lipid-rich diets (22). These factors can lead to increased mito-

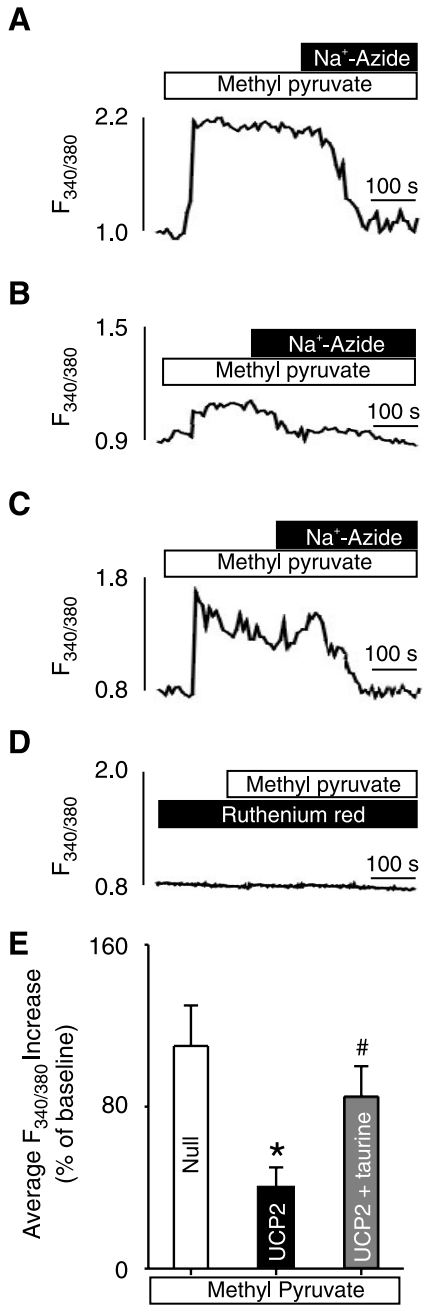

Fig. 8. UCP2-overexpressing mitochondria showed reduced mitochondrial Ca^{2+} concentration ($[Ca^{2+}]_m$) responsiveness to methyl pyruvate. Fluorescence ratios ($F_{340/380}$) induced by 20 mM methyl pyruvate. The typical sequence of additions was as follows: after a robust $[Ca^{2+}]_m$ response to methyl pyruvate (20 mM; open bar), sodium azide (3 mM; solid bar) was added in the presence of methyl pyruvate. Tracings are representative of data obtained using Ad-Null (*A*), Ad-UCP2 (*B*), and Ad-UCP2 + T mitochondria (*C*). *D*: a representative trace showing the effect of ruthenium red (10 μM) on Ad-UCP2 + T mitochondria. *E*: $[Ca^{2+}]_m$ response to methyl pyruvate, expressed as a percentage of the response before addition of methyl pyruvate in Ad-Null (open column; $n = 7$), Ad-UCP2 (solid column; $n = 6$), and Ad-UCP2 + T mitochondria (gray column; $n = 6$). *$P <$ 0.05 compared with Ad-Null-infected mitochondria; #$P < 0.05$ compared with Ad-UCP2-infected mitochondria.

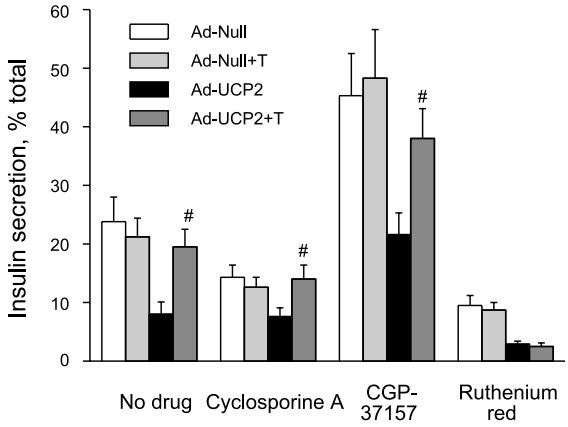

Fig. 9. Effect of taurine on GSIS at 15 mM glucose in Ad-UCP2-infected islets pretreated with cyclosporine A and CGP-37157 for 1 h and ruthenium red for 24 h. Insulin secretion is expressed as a percentage of total insulin content secreted. T, pretreatment with 0.3 mM taurine for 24 h. Symbols represent means ± SE; $n = 4–6$ for each mean. #$P < 0.05$ compared with Ad-UCP2-infected islets.

chondrial UCP2 protein expression. There is considerable evidence that mitochondrial activation in β-cells is critical for GSIS (29). For example, patients with mitochondrial DNA mutations exhibit impaired β-cell function (15, 27), and an estimated 98% of β-cell ATP is generated by mitochondrial oxidative metabolism (13). In addition, blockade of β-cell mitochondrial metabolism inhibits insulin secretion (4).

A normal plasma taurine level in gestating mothers is necessary for fetal β-cell development (6). Taurine may act on the rate of β-cell apoptosis and DNA synthesis (6) and may reduce β-cell sensitivity to nitric oxide (31). Although taurine increased GSIS in cultured rat fetal islets in an acute manner (9, 10), it was also reported to suppress GSIS in acutely isolated mouse islets (45). Therefore, the effect of taurine on GSIS remains the subject of controversy.

The present results showed that taurine pretreatment improved impaired GSIS in islets overexpressing UCP2. This effect was not so obvious in Ad-Null-infected islets in which GSIS was normal. Furthermore, taurine did not increase basal levels of insulin secretion in Ad-UCP2-infected islets in 3 mM glucose, indicating that taurine acts in a glucose-dependent manner. However, the ability of taurine to stimulate insulin secretion in response to high glucose may begin to operate at basal glucose concentrations, since the ATP/ADP ratio at 3 mM glucose was already ameliorated by taurine. The effect of taurine on GSIS does not appear to be due to taurine inhibiting UCP2 expression, as neither UCP2 upregulation induced by chronic high glucose exposure nor adenovirus-mediated UCP2 overexpression was affected by taurine (data not shown).

Overt K_{ATP} channel inhibition and the subsequent increase in $[Ca^{2+}]_c$ by the K_{ATP} channel blocker glibenclamide were observed in Ad-UCP2-infected islet cells. Therefore, it can be speculated that UCP2-overexpressing β-cells do not have any significant defect in the glucose-stimulated insulin secretory pathway downstream of K_{ATP} channel inhibition. These observations further imply that taurine stimulation of GSIS affects glucose metabolism, oxidation, and ATP generation, which are followed by K_{ATP} channel inhibition. The results of the DHA experiments indicate that enough ATP can be produced to inhibit channel activity if a sufficient amount of reducing equivalents is delivered to the electron transport system, regardless of the level of UCP2 expression. These studies also suggest that taurine is effective at certain sites in the TCA cycle where reducing equivalents are produced and the metabolic rate is influenced by $[Ca^{2+}]_m$. UCP2 overexpression may ultimately impair the activity of Ca^{2+}-sensitive dehydrogenases in the TCA cycle (29) because of UCP2-induced decreases in mitochondrial membrane potential (7), the driving force for increasing $[Ca^{2+}]_m$. We demonstrated that taurine pretreatment significantly restored the methyl pyruvate-mediated increase in $[Ca^{2+}]_m$ in Ad-UCP2-infected mitochondria. It was recently reported that taurine could be incorporated into mitochondria time dependently through a putative mitochondrial taurine transporter (44). The cytosolic medium containing the isolated mitochondria for our $[Ca^{2+}]_m$ measurements did not contain taurine, strongly suggesting that intramitochondrial taurine participated in the methyl pyruvate-mediated $[Ca^{2+}]_m$ elevation in Ad-UCP2-infected mitochondria. In addition, suppression of the uniporter-mediated Ca^{2+} influx by ruthenium red abolished the taurine effect, suggesting that taurine increases $[Ca^{2+}]_m$ through Ca^{2+} uniporter activation, consistent with observations in liver (34) and neuronal (21) mitochondria. Ca^{2+} uptake into rat liver mitochondria mediated by the high-affinity (5–20 μM) Ca^{2+} uniporter is reported to be stimulated by taurine (33) at a physiological intracellular taurine concentration (10 mM), increasing the rate almost twofold (34).

In the present study, the Na^+/Ca^{2+} exchanger and PTP did not appear to be involved in the actions of taurine, since their antagonists did not inhibit taurine action. The Na^+/Ca^{2+} exchanger mechanism is dominant in the mitochondria of excitable tissues, such as heart, brain, and hormone-releasing cells, where rapid release of Ca^{2+} may be important to mediate rapid changes in $[Ca^{2+}]_m$. In contrast, the Ca^{2+}/H^+ exchanger mechanism is dominant in liver and kidney, which are major tissues involved in clearance of metal ions from the body (37). Blocking β-cell Na^+/Ca^{2+} exchangers has been reported to increase GSIS (12), whereas the reverse is true in the case of PTP blockage by the immunosuppressive drug CysA (23). This difference in regulation of insulin secretion might be due to the distinct physiological roles of these compounds, with PTP being intimately involved in other important functions such as apoptosis (37).

Although the sites to which taurine binds to modify Ca^{2+} uniporter function are yet to be identified, taurine has been shown to decrease the fluidity of biological membranes in the presence of Ca^{2+} (32). Thus taurine might alter the interaction of the mitochondrial Ca^{2+} uniporter with the lipid bilayer, thereby affecting uniporter kinetic behavior (34). However, it is also possible that taurine acts directly on UCP2 activity.

In conclusion, the results presented here suggest that taurine ameliorates glucose sensitivity in UCP2-overexpressing β-cells, thereby increasing GSIS. It appears that taurine acts through the mitochondrial Ca^{2+} uniporter to increase $[Ca^{2+}]_m$. These data suggest that restoration of plasma taurine level could be critical in preventing or improving obesity-related β-cell dysfunction as well as many diabetic complications.

GRANTS

This work was supported by grant no. R13-2002-028-01003-0 from the Basic Research Program of the Korea Science and Engineering Foundation for the Chronic Disease Research Center at Keimyung University.

REFERENCES

1. **Asfari M, Janjic D, Meda P, Li G, Halban PA, and Wollheim CB.** Establishment of 2-mercaptoethanol-dependent differentiated insulin-secreting cell lines. *Endocrinology* 130: 167–178, 1992.
2. **Ashcroft FM and Gribble FM.** ATP-sensitive K^+ channels and insulin secretion: their role in health and disease. *Diabetologia* 42: 903–919, 1999.
3. **Bae JH, Park JW, and Kwon TK.** Ruthenium red, inhibitor of mitochondrial Ca^{2+} uniporter, inhibits curcumin-induced apoptosis via the prevention of intracellular Ca^{2+} depletion and cytochrome *c* release. *Biochem Biophys Res Commun* 303: 1073–1079, 2003.
4. **Best L.** Glucose and alpha-ketoisocaproate induce transient inward currents in rat pancreatic beta cells. *Diabetologia* 40: 1–6, 1997.
5. **Boss O, Muzzin P, and Giacobino JP.** The uncoupling proteins, a review. *Eur J Endocrinol* 139: 1–9, 1998.
6. **Boujendar S, Reusens B, Merezak S, Ahn MT, Arany E, Hill D, and Remacle C.** Taurine supplementation to a low protein diet during foetal and early postnatal life restores a normal proliferation and apoptosis of rat pancreatic islets. *Diabetologia* 45: 856–866, 2002.
7. **Chan CB, De Leo D, Joseph JW, McQuaid TS, Ha XF, Xu F, Tsushima RG, Pennefather PS, Salapatek AM, and Wheeler MB.** Increased uncoupling protein-2 levels in beta-cells are associated with impaired glucose-stimulated insulin secretion: mechanism of action. *Diabetes* 50: 1302–1310, 2001.
8. **Chan CB, MacDonald PE, Saleh MC, Johns DC, Marban E, and Wheeler MB.** Overexpression of uncoupling protein 2 inhibits glucose-stimulated insulin secretion from rat islets. *Diabetes* 48: 1482–1486, 1999.
9. **Cherif H, Reusens B, Ahn MT, Hoet JJ, and Remacle C.** Effects of taurine on the insulin secretion of rat fetal islets from dams fed a low protein diet. *J Endocrinol* 159: 341–348, 1998.
10. **Cherif H, Reusens B, Dahri S, Remacle C, and Hoet JJ.** Stimulatory effects of taurine on insulin secretion by fetal rat islets cultured in vitro. *J Endocrinol* 151: 501–506, 1996.
11. **Choi YK, Kim YJ, Park HS, Choi K, Paik SG, Lee YI, and Park JG.** Suppression of glomerulosclerosis by adenovirus-mediated IL-10 expression in the kidney. *Gene Ther* 10: 559–568, 2003.
12. **Dufer M, Krippeit-Drews P, Lembert N, Idahl LA, and Drews G.** Diabetogenic effect of cyclosporine A is mediated by interference with mitochondrial function of pancreatic B-cells. *Mol Pharmacol* 60: 873–879, 2001.
13. **Erecinska M, Bryla J, Michalik M, Meglasson MD, and Nelson D.** Energy metabolism in islets of Langerhans. *Biochim Biophys Acta* 1101: 273–295, 1992.
14. **Fleury C, Neverova M, Collins S, Raimbault S, Champigny O, Levi-Meyrueis C, Bouillaud F, Seldin MF, Surwit RS, Ricquier D, and Warden CH.** Uncoupling protein-2: a novel gene linked to obesity and hyperinsulinemia. *Nat Genet* 15: 269–272, 1997.
15. **Gerbitz KD, Gempel K, and Brdiczka D.** Mitochondria and diabetes. Genetic, biochemical, and clinical implications of the cellular energy circuit. *Diabetes* 45: 113–126, 1996.
16. **Giannoukakis N, Rudert WA, Ghivizzani SC, Gambotto A, Ricordi C, Trucco M, and Robbins PD.** Adenoviral gene transfer of the interleukin-1 receptor antagonist protein to human islets prevents IL-1β-induced beta-cell impairment and activation of islet cell apoptosis in vitro. *Diabetes* 48: 1730–1736, 1999.
17. **Graham FL and van der Eb AJ.** A new technique for the assay of infectivity of human adenovirus 5 DNA. *Virology* 52: 456–467, 1973.
18. **Guerini D, Prati E, Desai U, Nick HP, Flammer R, Gruninger S, Cumin F, Kaleko M, Connelly S, and Chiesi M.** Uncoupling of protein-3 induces an uncontrolled uncoupling of mitochondria after expression in muscle derived L6 cells. *Eur J Biochem* 269: 1373–1381, 2002.
19. **Gunter TE, Buntinas L, Sparagna G, Eliseev R, and Gunter K.** Mitochondrial calcium transport: mechanisms and functions. *Cell Calcium* 28: 285–296, 2000.
20. **Huxtable RJ.** Physiological actions of taurine. *Physiol Rev* 72: 101–163, 1992.
21. **Kuriyama K, Muratmatsu M, Nakagawa K, and Kakita K.** Modulating role of taurine on release of neurotransmitters and calcium transport in excitable tissues. In: *Taurine and Neurological Disorders*, edited by Barbeau A and Huxtable RJ. New York: Raven, 1978, p. 201–216.
22. **Lameloise N, Muzzin P, Prentki M, and Assimacopoulos-Jeannet F.** Uncoupling protein 2: a possible link between fatty acid excess and impaired glucose-induced insulin secretion? *Diabetes* 50: 803–809, 2001.
23. **Lee B, Miles PD, Vargas L, Luan P, Glasco S, Kushnareva Y, Kornbrust ES, Grako KA, Wollheim CB, Maechler P, Olefsky JM, and Anderson CM.** Inhibition of mitochondrial Na^+-Ca^{2+} exchanger increases mitochondrial metabolism and potentiates glucose-stimulated insulin secretion in rat pancreatic islets. *Diabetes* 52: 965–973, 2003.
24. **Lembert N, Joos HC, Idahl LA, Ammon HP, and Wahl MA.** Methyl pyruvate initiates membrane depolarization and insulin release by metabolic factors other than ATP. *Biochem J* 354: 345–350, 2001.
25. **Li LX, Skorpen F, Egeberg K, Jorgensen IH, and Grill V.** Uncoupling protein-2 participates in cellular defense against oxidative stress in clonal beta-cells. *Biochem Biophys Res Commun* 282: 273–277, 2001.
26. **Lombardini JB.** Effects of taurine and mitochondrial metabolic inhibitors on ATP-dependent Ca^{2+} uptake in synaptosomal and mitochondrial subcellular fractions of rat retina. *J Neurochem* 51: 200–205, 1988.
27. **Maassen JA and Kadowaki T.** Maternally inherited diabetes and deafness: a new diabetes subtype. *Diabetologia* 39: 375–382, 1996.
28. **MacDonald MJ and Brown LJ.** Calcium activation of mitochondrial glycerol phosphate dehydrogenase restudied. *Arch Biochem Biophys* 326: 79–84, 1996.
29. **Maechler P, Kennedy ED, Pozzan T, and Wollheim CB.** Mitochondrial activation directly triggers the exocytosis of insulin in permeabilized pancreatic beta-cells. *EMBO J* 16: 3833–3841, 1997.
30. **McCormack JG, Halestrap AP, and Denton RM.** Role of calcium ions in regulation of mammalian intramitochondrial metabolism. *Physiol Rev* 70: 391–425, 1990.
31. **Merezak S, Hardikar AA, Yajnik CS, Remacle C, and Reusens B.** Intrauterine low protein diet increases fetal beta-cell sensitivity to NO and IL-1 beta: the protective role of taurine. *J Endocrinol* 171: 299–308, 2001.
32. **Nakashima T, Shima T, Sakai M, Yama H, Mitsuyoshi H, Inaba K, Matsumoto N, Sakamoto Y, Kashima K, and Nishikawa H.** Evidence of a direct action of taurine and calcium on biological membranes. A combined study of ^{31}P-nuclear magnetic resonance and electron spin resonance. *Biochem Pharmacol* 52: 173–176, 1996.
33. **Palmi M, Fusi F, Youmbi G, Frosini M, Bianchi L, Della Corte L, Sgaragli GP, and Tipton KF.** Effects of taurine and structurally related analogues on Ca^{2+} uptake and respiration rate in rat liver mitochondria. *Adv Exp Med Biol* 403: 117–124, 1996.
34. **Palmi M, Youmbi GT, Fusi F, Sgaragli GP, Dixon HB, Frosini M, and Tipton KF.** Potentiation of mitochondrial Ca^{2+} sequestration by taurine. *Biochem Pharmacol* 58: 1123–1131, 1999.
35. **Park EJ, Bae JH, Kim SY, Lim JG, Baek WK, Kwon TK, Suh SI, Park JW, Lee IK, Ashcroft FM, and Song DK.** Inhibition of ATP-sensitive K^+ channels by taurine through a benzamido-binding site on sulfonylurea receptor 1. *Biochem Pharmacol* 67: 1089–1096, 2004.
36. **Patane G, Anello M, Piro S, Vigneri R, Purrello F, and Rabuazzo AM.** Role of ATP production and uncoupling protein-2 in the insulin secretory defect induced by chronic exposure to high glucose or free fatty acids and effects of peroxisome proliferator-activated receptor-γ inhibition. *Diabetes* 51: 2749–2756, 2002.
37. **Pfeiffer DR, Gunter TE, Eliseev R, Broekemeier KM, and Gunter KK.** Release of Ca^{2+} from mitochondria via the saturable mechanisms and the permeability transition. *IUBMB Life* 52: 205–212, 2001.
38. **Pralong WF, Bartley C, and Wollheim CB.** Single islet beta-cell stimulation by nutrients: relationship between pyridine nucleotides, cytosolic Ca^{2+} and secretion. *EMBO J* 9: 53–60, 1990.
39. **Rutter GA, Burnett P, Rizzuto R, Brini M, Murgia M, Pozzan T, Tavare JM, and Denton RM.** Subcellular imaging of intramitochondrial Ca^{2+} with recombinant targeted aequorin: significance for the regulation of pyruvate dehydrogenase activity. *Proc Natl Acad Sci USA* 93: 5489–5494, 1996.
40. **Scheffler IE.** Mitochondrial electron transport and oxidative phosphorylation. In: *Mitochondria.* New York: Wiley-Liss, 1999, p. 141–245.
41. **Schultz V, Sussman I, Bokvist K, and Tornheim K.** Bioluminometric assay of ADP and ATP at high ATP/ADP ratios: assay of ADP after enzymatic removal of ATP. *Anal Biochem* 215: 302–304, 1993.
42. **Sebring LA and Huxtable RJ.** Taurine modulation of calcium binding to cardiac sarcolemma. *J Pharmacol Exp Ther* 232: 445–451, 1985.
43. **Song DK, Park WK, Bae JH, Park MK, Kim SJ, Ho WK, and Earm YE.** Reduced dihydroxyacetone sensitivity and normal sensitivity to

glyceraldehyde and oxidizing agent of ATP-sensitive K^+ channels of pancreatic beta cells in NIDDM rats. *J Korean Med Sci* 12: 286–292, 1997.

44. **Suzuki T, Wada T, Saigo K, and Watanabe K.** Taurine as a constituent of mitochondrial tRNAs: new insights into the functions of taurine and human mitochondrial diseases. *EMBO J* 21: 6581–6589, 2002.
45. **Tokunaga H, Yoneda Y, and Kuriyama K.** Streptozotocin-induced elevation of pancreatic taurine content and suppressive effect of taurine on insulin secretion. *Eur J Pharmacol* 87: 237–243, 1983.
46. **Weber M, Deng S, Kucher T, Shaked A, Ketchum RJ, and Brayman KL.** Adenoviral transfection of isolated pancreatic islets: a study of programmed cell death (apoptosis) and islet function. *J Surg Res* 69: 23–32, 1997.
47. **Wu L, Nicholson W, Knobel SM, Steffner RJ, May JM, Piston DW, and Powers AC.** Oxidative stress is a mediator of glucose toxicity in insulin-secreting pancreatic islet cell lines. *J Biol Chem* 279: 12126–12134, 2004.
48. **Zhang CY, Baffy G, Perret P, Krauss S, Peroni O, Grujic D, Hagen T, Vidal-Puig AJ, Boss O, Kim YB, Zheng XX, Wheeler MB, Shulman GI, Chan CB, and Lowell BB.** Uncoupling protein-2 negatively regulates insulin secretion and is a major link between obesity, beta cell dysfunction, and type 2 diabetes. *Cell* 105: 745–755, 2001.
49. **Zhou YP and Grill V.** Long term exposure to fatty acids and ketones inhibits B-cell functions in human pancreatic islets of Langerhans. *J Clin Endocrinol Metab* 80: 1584–1590, 1995.
50. **Zhou YP, Marlen K, Palma JF, Schweitzer A, Reilly L, Gregoire FM, Xu GG, Blume JE, and Johnson JD.** Overexpression of repressive cAMP response element modulators in high glucose and fatty acid-treated rat islets. A common mechanism for glucose toxicity and lipotoxicity? *J Biol Chem* 278: 51316–51323, 2003.